[8]Martinelli, L., Jameson, A., and Grasso, F., "A Multigrid Method for Navier–Stokes Equations," AIAA Paper 86-0208, Jan. 1986.

[9]Lee, S. L., and Damodaran, M., "Aerodynamic Design of Transonic Airfoils Using Simulated Annealing and Navier–Stokes Equations," AIAA Paper 2000-0782, Jan. 2000.

[10]Aarts, E., and Korst, J., *Simulated Annealing and Boltzmann Machines, A Stochastic Approach to Combinatorial Optimization and Neural Computing*, Wiley, New York, 1989, p. 12.

[11]Bhandarkar, S. M., and Machaka, S., "Chromosome Reconstruction from Physical Maps Using a Cluster of Workstations," *Journal of Supercomputing*, Vol. 11, No. 1, 1997, pp. 61–87.

[12]Eyi, S., and Lee, K. D., "Aerodynamic Design via Optimization," *Journal of Aircraft*, Vol. 29, No. 6, 1992, pp. 1012–1019.

P. Givi
Associate Editor

Improved Formulation for Boundary-Layer-Type Flows

H. Dumitrescu* and V. Cardoş†
Romanian Academy, RO 70700 Bucharest, Romania

I. Introduction

THE matching of a viscous boundary-layer calculation with a inviscid flowfield solution is not without its difficulties. It is well known that when the pressure gradient is prescribed, the wall shear stress approaches zero in a singular fashion at separation, which invariably gives rise to problems on numerical convergence there.[1] This is particularly true for an inviscid shear layer near the edge of the boundary layer. Traditional boundary-layer methods neglect this layer, and even when it is considered, it is assumed that the flowfield properties approach the inviscid values at the boundary-layer edge with a zero slope. This assumption is particularly poor for lower Reynolds numbers and at separation approaching where the boundary layer is thickening. If the boundary-layer solution does not match the inviscid solution well, then surface properties such as skin-friction and heat transfer rates are not calculated accurately. Therefore, this Note develops a new method for better matching inviscid–boundary-layer flowfields.

II. New Boundary-Layer Model

The traditional method of calculating the boundary-layer properties assumes a distinct hierarchy between the viscous and inviscid flowfields. That is, an inviscid flowfield is first calculated neglecting the boundary layer, and the inviscid properties on the body surface are subsequently used as edge conditions for the boundary-layer solutions. However, for the boundary layers in adverse pressure gradients, a shear layer exists near the surface in the inviscid solution, and the inviscid properties at the edge of the boundary layer can be significantly different from those on the surface. For these flowfields, the boundary-layer solution will yield more accurate results if the inviscid properties at a distance from the surface are used as edge conditions. In this case, although some boundary-layer methods, take into account the inviscid shear layer, they assume the flowfield properties approach the inviscid values at the boundary-layer edge with a zero slope (Fig. 1a).

The method presented here uses a new form of the boundary-layer equations that matches exactly all of the properties except the normal velocity component (Fig. 1b). The normal velocity can also be matched by means of a usual iterative process.[2]

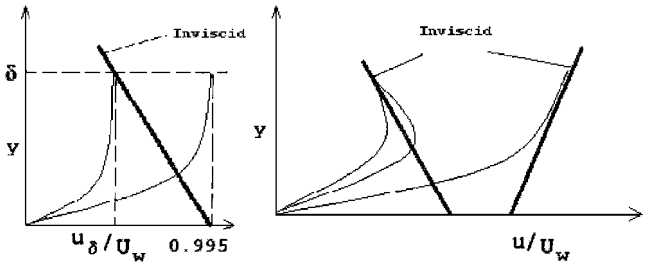

a) Classical method b) Present method

Fig. 1 Inviscid and boundary-layer solution matching.

To illustrate the operation of this procedure more clearly, we consider the specific case of steady, two-dimensional, incompressible, laminar flow. The inviscid equations for this case are as follows.

The continuity equation:

$$\frac{\partial U}{\partial x} + \frac{\partial V}{\partial x} = 0 \tag{1}$$

The x-momentum equation:

$$U\frac{\partial U}{\partial x} + V\frac{\partial U}{\partial y} = -\frac{1}{\rho}\frac{\partial P}{\partial x} \tag{2}$$

The y-momentum equation:

$$U\frac{\partial V}{\partial x} + V\frac{\partial V}{\partial y} = -\frac{1}{\rho}\frac{\partial P}{\partial y} \tag{3}$$

They are subjected to the boundary conditions

$$y = 0, \qquad V(x, 0) = 0 \tag{4}$$

$$y \to \infty, \qquad U^2 + V^2 = U_\infty^2 + V_\infty^2 \tag{5}$$

Also, the viscous flowfield is described by the following classical boundary-layer equations.

The continuity equation:

$$\frac{\partial u}{\partial x} + \frac{\partial v}{\partial x} = 0 \tag{6}$$

The x-momentum equation:

$$u\frac{\partial u}{\partial x} + v\frac{\partial u}{\partial y} - \nu\frac{\partial^2 u}{\partial y^2} = -\frac{1}{\rho}\frac{\partial P}{\partial x} \tag{7}$$

The y-momentum equation:

$$0 = -\frac{1}{\rho}\frac{\partial P}{\partial y} \tag{8}$$

These have the boundary conditions

$$y = 0, \qquad u(x, 0) = v(x, 0) = 0 \tag{9}$$

$$y \to \infty, \qquad u = U(x, 0) = U_w \tag{10}$$

The mathematical difficulties of the problem are associated primarily with the mixed elliptic and parabolic types of the equations and the presence of strong interactions at separation. In this context, note that if the boundary-layer solution u cannot match exactly the inviscid solution U (that is, both in magnitude and slope) at the outer boundary, then a smooth solution is not possible at separation. An appropriate solution to separation requires the proper matching of the boundary-layer solution with the inviscid solution, that is,

$$u = U(x, y), \qquad v = V(x, y) \qquad \text{for} \qquad y \geq \delta \tag{11}$$

The boundary conditions given by Eq. (11) will match exactly the boundary-layer flowfield with the inviscid flowfield, as shown in Fig. 1b. Now, because $\partial v/\partial y$ is the highest y derivative on v, the boundary conditions imposed on v given by Eqs. (9) and (11) are overspecified, and this enables the solution of an additional unknown. That unknown introduced here is the inviscid transpiration

Received 19 April 2001; revision received 1 September 2001; accepted for publication 27 September 2001. Copyright © 2002 by the American Institute of Aeronautics and Astronautics, Inc. All rights reserved. Copies of this paper may be made for personal or internal use, on condition that the copier pay the $10.00 per-copy fee to the Copyright Clearance Center, Inc., 222 Rosewood Drive, Danvers, MA 01923; include the code 0001-1452/02 $10.00 in correspondence with the CCC.

*Professor and Senior Researcher, Caius Iacob Institute of Applied Mathematics, P.O. Box 1-24.

†Senior Researcher, Caius Iacob Institute of Applied Mathematics, P.O. Box 1-24.

velocity at the wall, $V_w(x)$, which accounts for the mass defect in the boundary layer. Now, the wall condition becomes

$$V(x, 0) = V_w(x) \qquad \text{at} \qquad y = 0 \tag{12}$$

Equation (12) replaces Eq. (4) as a boundary condition for the new inviscid solution, that is, for the equivalent inviscid flow.

An exact representation of the flowfield through the region shown in Fig. 1b is given by a solution of the Navier–Stokes equations. However, the solution of the equations governing the outer-inviscid flow will provide a close approximation of the exact solution when $y > \delta$. Thus, Eqs. (1) and (6) may be integrated from $y = 0$ to δ to give

$$V_\delta - V_0 = -\int_0^\delta \frac{\partial U}{\partial x}\,\mathrm{d}y \tag{13}$$

$$v_\delta - v_0 = -\int_0^\delta \frac{\partial u}{\partial x}\,\mathrm{d}y \tag{14}$$

where the subscripts indicate evaluation at the limits of integration. Because the two solutions may be taken to coincide for $y \geq \delta$, we specify $V_\delta = v_\delta$. If $V_0 = V_w(x)$ and $v_0 = 0$, then Eqs. (13) and (14) can be combined to give

$$V_w(x) = \frac{\mathrm{d}}{\mathrm{d}x}\int_0^\delta (U - u)\,\mathrm{d}y \tag{15}$$

Equation (15), which relates the two hypothetical solutions, will serve as a starting point for the solution technique in the boundary-layer field. Thus, Eq. (2) is used to replace the right-hand side of Eq. (7), with V for the equivalent inviscid flow (EIF) given by

$$V_{\mathrm{EIF}}(x, y) = V_w(x) - \int_0^y \frac{\partial U}{\partial x}\,\mathrm{d}y \tag{16}$$

Furthermore, to have a full term-by-term correspondence between the two sides of the x-momentum equation, an artificial viscous term is added to the inviscid right-hand side. This term, which is generally small, ensures an exact matching of $u(x, y)$ with $U(x, y)$. Therefore, the new boundary-layer equation is obtained as

$$u\frac{\partial u}{\partial x} + v\frac{\partial u}{\partial y} - \nu\frac{\partial^2 u}{\partial y^2} = U\frac{\partial U}{\partial x} + V_{\mathrm{EIF}}\frac{\partial U}{\partial y} - \nu\frac{\partial^2 U}{\partial y^2} \tag{17}$$

with the outer boundary condition

$$y \geq \delta, \qquad u = U(x, y), \qquad v = V_{\mathrm{EIF}}(x, y) \tag{18}$$

Equations (6) and (15–17) with the boundary conditions given by Eqs. (9) and (18) make up the improved boundary-layer formulation. The additional terms included in the inviscid right-hand side of Eq. (17) permit the boundary-layer solution u to match the inviscid solution U without any fictitious boundary condition imposed on $\partial u/\partial y$ at the outer boundary. If y is sufficiently large, there will be an exact matching of u with $U(x, y)$ and v with $V_{\mathrm{EIF}}(x, y)$. Thus, the precise definition of the boundary-layer thickness is not required, this being consistent with the precision of the computation chosen.

At the other hand, the free outer boundary condition given by Eq. (18) provides an asymptotic matching of the viscous and inviscid flowfields, in contrast with the fixed condition given by Eq. (10). This natural behavior permits to obtain regular solutions for local small-scale separation conditions, where the classical boundary-layer equations are singular.

The transpiration velocity, Eq. (15), obtained as part of the boundary-layer solution can be then used as a boundary condition to calculate a new inviscid solution. Thus, some of the viscous–inviscid interaction is included in the initial boundary-layer calculations.

III. Numerical Results and Discussion

The method described earlier is applied to the special case of linearly retarded flow over a flat plate (Howarth flow) with a superimposed constant shear flow ($\alpha = \pm 5$, $Re = 10^4$), which gives directly the inviscid velocity field $U(x, y)$, avoiding iterations of the inviscid–boundary-layer solutions. Thus, the resulting inviscid flowfield is given by

$$U/U_\infty = (1 - x/L)/(1 \pm \alpha y/L) \tag{19}$$

Once the matching method is checked for this particular case, it can be applied to more general cases, including full inviscid–boundary-layer interaction.

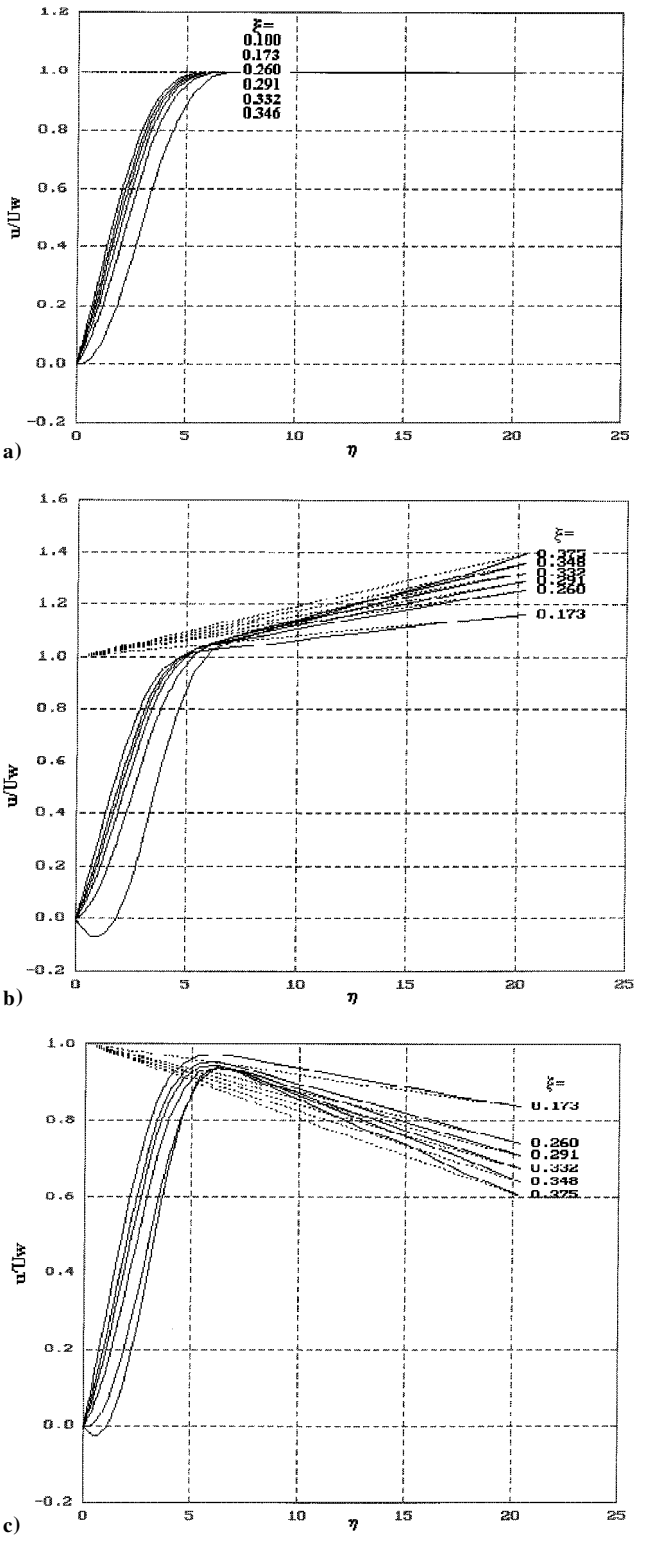

Fig. 2 Velocity profiles in the boundary layer computed by a) the standard method ($\partial U/\partial y = 0$) and b) accelerated shear flow ($\alpha = +5.0$) and c) retarded shear flow ($\alpha = -5.0$) by the present method ($\partial U/\partial y \neq 0$).

We use the similarity variables for the standard boundary-layer problem

$$\eta = (U_w/\nu x)^{\frac{1}{2}} y, \qquad \xi = (x/L)^{\frac{1}{2}} \tag{20}$$

$$f = \int_0^\eta \frac{u}{U_w}\,\mathrm{d}\eta, \qquad F = F_w(\xi) + \int_0^\eta \frac{U}{U_w}\,\mathrm{d}\eta \tag{21}$$

Consequently, Eqs. (6) and (15–17) are transformed to

$$f''' + \frac{1}{2}ff'' - \frac{\xi}{2}[f'f'_\xi - f_\xi f''] - \frac{\xi}{2}\frac{1}{U_w}\frac{\mathrm{d}U_w}{\mathrm{d}\xi}\left(f'^2 - \frac{1}{2}ff''\right)$$
$$= F''' + \frac{1}{2}FF'' - \frac{\xi}{2}[F'F'_\xi - F_\xi F'']$$
$$- \frac{\xi}{2}\frac{1}{U_w}\frac{\mathrm{d}U_w}{\mathrm{d}\xi}\left(F'^2 - \frac{1}{2}FF''\right) \tag{22}$$

$$F_w = \int_0^{\eta_\delta} (f' - F')\,\mathrm{d}\eta \tag{23}$$

$$\frac{V_w\sqrt{Re_x}}{U_0} = -\frac{1}{2}\frac{\mathrm{d}}{\mathrm{d}\xi}\left(\xi\sqrt{\frac{U_w}{U_0}F_w}\right) \tag{24}$$

Here the primes denote differentiation with respect to η and subscript ξ the differentiation with respect to ξ.

The term $F_w(\xi)$ is the mass flux at the wall in the equivalent inviscid flow to account for the boundary-layer mass defect, and it is generally negative. The boundary conditions given by Eqs. (9) and (18) can also be written as

$$\eta = 0, \qquad f(\xi, 0) = f'(\xi, 0) = 0 \tag{25}$$

$$\eta = \eta_\delta, \qquad f = F, \qquad f' = F' \tag{26}$$

The inviscid solution gives $F'(\xi, \eta)$ and the boundary-layer solution provides $F_w(\xi)$. The partial differential equation given by Eq. (22) is numerically solved by using Keller's two-point finite difference method described in Ref. 3.

A comparison between the velocity profiles in the boundary layer predicted by the standard boundary-layer method and the present boundary-layer method for the case considered is shown in Fig. 2. The value chosen for η_δ is consistent with the precision of computation of 10^{-5}. In Fig. 3, a comparison is shown between the wall shear stress expressed in the form of the skin-friction coefficient $\frac{1}{2}C_f Re_x^{1/2}$ as predicted by the two methods. It can be seen that the standard method breaks down at separation, whereas with the present method, solutions were obtained that passed smoothly through the point of separation into the separated region, with no evidence of the type of singular behavior at separation that Goldstein[4] had shown to occur in the direct problem.

Unlike the classical boundary-layer methods, which require that the velocity (or pressure) distribution on the body surface to be known $[U_w(x)]$, for the present method the inviscid velocity field $[U(x, y)]$ in close vicinity of body is assumed known. For this reason the direct boundary-layer method described in this Note can be used conveniently in conjunction with a field method for the inviscid flow. The method is limited to local small-scale separation, such as the trailing-edge separation on the upper side of airfoils. The approach of the flows with massive separation, such as the leading-edge separation of airfoils at high angles of attack, requires more involved methods, such as Navier–Stokes and triple-deck methods.[5]

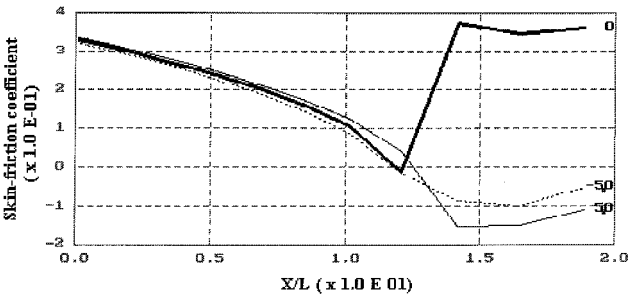

Fig. 3 Skin-friction coefficient computed by standard method ($\partial U/\partial y = 0$) (- - - -) and present method ($\partial U/\partial y \neq 0$) (- - - -).

IV. Conclusions

The solutions of the classical boundary-layer equations with adverse pressure gradient often terminate in the form of a Goldstein[4] singularity. A new boundary-layer formulation that avoids this singularity has been presented. The method includes a local interaction between the viscous wall layer and the external inviscid region in the initial boundary-layer solution. This local interaction strategy has been applied successfully to describe flows with local small-scale separation called marginally separated boundary layers. Some results show that flows with small amount of separation can be calculated by direct boundary-layer technique. Theoretically, the method enables us to look systematically into the complicated boundary-layer flow behavior resulting from the strong interactions.

References

[1] Wehrle, V. A., "Determination of the Separation Point in Laminar Boundary-Layer Flows," *AIAA Journal*, Vol. 24, No. 10, 1986, pp. 1636–1641.

[2] Veldman, A. E. P., Lindhout, J. P. F., deBoer, E., and Somers, M. A. M., "A Simulation Method for Strongly Interacting Viscous Transonic Flow," *Numerical and Physical Aspects of Aerodynamic Flows IV*, Springer-Verlag, New York, 1990, pp. 37–51.

[3] Cebeci, T., and Bradshaw, P., *Physical and Computational Aspects of Convective Heat Transfer*, Springer-Verlag, New York, 1984, pp. 385–395.

[4] Goldstein, S., "On Laminar Boundary-Layer Flow Near a Position of Separation," *Quarterly Journal of Mechanics and Applied Mathematics*, Vol. 1, 1948, pp. 43–51.

[5] Veldman, A. E. P., "Matched Asymptotic Expansions and the Numerical Treatment of Viscous–Inviscid Interaction," *Journal of Engineering Mathematics*, Vol. 39, No. 1/4, 2001, pp. 189–206.

S. K. Aggarwal
Associate Editor